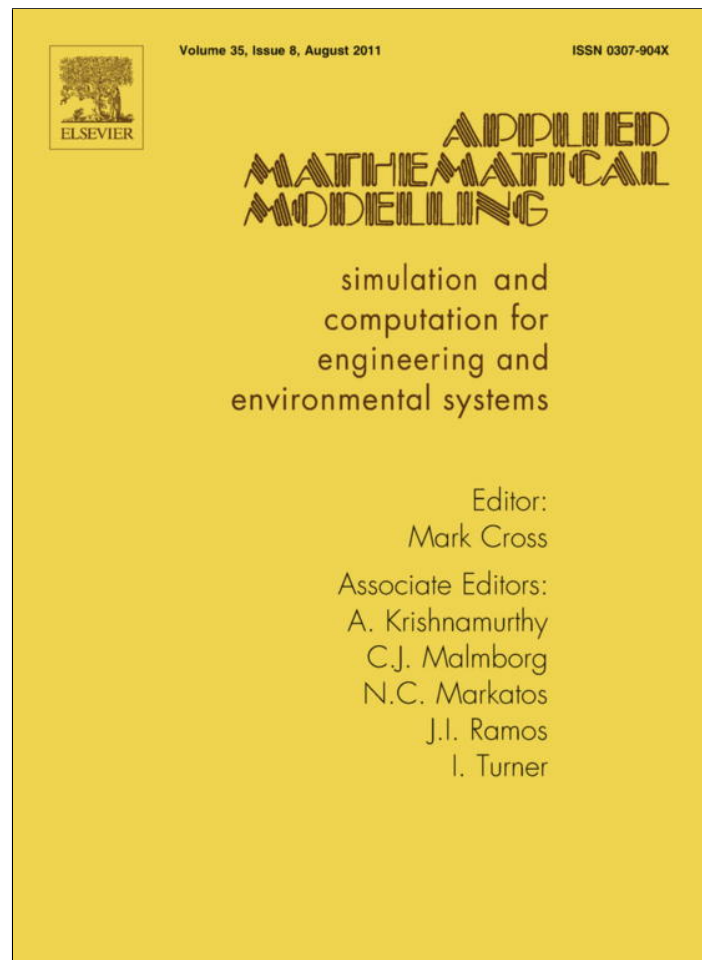


Provided for non-commercial research and education use.
Not for reproduction, distribution or commercial use.



This article appeared in a journal published by Elsevier. The attached copy is furnished to the author for internal non-commercial research and education use, including for instruction at the authors institution and sharing with colleagues.

Other uses, including reproduction and distribution, or selling or licensing copies, or posting to personal, institutional or third party websites are prohibited.

In most cases authors are permitted to post their version of the article (e.g. in Word or Tex form) to their personal website or institutional repository. Authors requiring further information regarding Elsevier's archiving and manuscript policies are encouraged to visit:

<http://www.elsevier.com/copyright>



Contents lists available at ScienceDirect

Applied Mathematical Modelling

journal homepage: www.elsevier.com/locate/apm

Optimal control of ice formation in living cells during freezing[☆]

N.D. Botkin, K.-H. Hoffmann, V.L. Turova^{*}

Technische Universität München, Zentrum Mathematik, Boltzmannstr. 3, 85748 Garching b. München, Germany

ARTICLE INFO

Article history:

Received 30 November 2009

Received in revised form 26 January 2011

Accepted 3 February 2011

Available online 26 February 2011

Keywords:

Cryopreservation

Cooling rate differential game

Value function

Optimal control

Finite-difference scheme

ABSTRACT

A mathematical model of ice formation in living cells during freezing is considered. Application of appropriate averaging techniques to partial differential equations describing the dynamics of water–ice phase transitions reduces spatially distributed relations to several ordinary differential equations with control parameters and uncertainties. Such equations together with an objective functional which expresses the difference between the amount of ice in the extracellular and intracellular liquids are treated as a differential game where the aim of the control is to maximize the objective functional and the aim of the disturbance is opposite. A stable finite-difference scheme for computing the value function is developed. Based on the computed value function, optimal controls are designed to produce cooling protocols ensuring simultaneous freezing inside and outside of living cells. Such a regime balances the pressures inside and outside of cells, which may prevent cells from injuring.

© 2011 Elsevier Inc. All rights reserved.

1. Introduction

Numerous modern medical technologies involve freezing and thawing out small tissue samples in such a manner that the cells preserve their functional properties. Optimization and control are necessary here because of several competitive effects of cooling. For example, a slow cooling causes freezing of the extracellular fluid, whereas the intracellular fluid remains unfrozen for a while. This results in large stresses that can violate the integrity of cell membranes. Slow cooling rates can also lead to an increase in the concentration of salt in the extracellular solution, which may cause dehydration and shrinkage of cells due to osmotic outflow through the cell membrane. If cooling is rapid, the water inside the cell forms small, irregularly-shaped ice crystals (dendrites) that are relatively unstable. If frozen cells are subsequently thawed out too slowly, dendrites will aggregate to form larger, more stable crystals that may cause damage (see [1,2] for thermodynamic models of intracellular ice nucleation and crystal growth). Maximum viability is obtained by cooling at a rate in a transition zone in which the combined effect of both these mechanisms is minimized (for physical aspects of cryopreservation see a comprehensive review [3]).

Thus, mathematical models describing the processes of freezing and thawing along with optimization problems are to be formulated. Such models basically utilize partial differential equations that describe the dynamics of phase transitions. Paper [4] is a pioneering work on phase field models related to solidification problems. It implements the idea to introduce a phase field variable that describes the volume fraction of the liquid phase at each spatial point and changes

[☆] The work was supported by German Research Society (DFG), Project SPP 1253.

^{*} Corresponding author. Tel.: +49 8928916828; fax: +49 8928916845.

E-mail addresses: botkin@ma.tum.de (N.D. Botkin), hoffmann@ma.tum.de (K.-H. Hoffmann), turova@ma.tum.de (V.L. Turova).

URLs: <http://www-m6.ma.tum.de/Lehrstuhl/NikolaiBotkin> (N.D. Botkin), <http://www-m6.ma.tum.de/Lehrstuhl/KarlHeinzHoffmann> (K.-H. Hoffmann), <http://www-m6.ma.tum.de/Lehrstuhl/VarvaraTurova> (V.L. Turova).

sharply but smoothly over the solidification front. Thermodynamical arguments applied to the Landau–Ginzburg type free energy result in a parabolic PDE system for the temperature and the phase field variable. The existence of global solutions is proved and an asymptotic analysis is performed in the case of Gibbs–Thomson conditions where the freezing temperature depends on the surface tension and the mean curvature of the interface. Paper [5] proposes a phase field model describing effects associated with supercooling. The model contains a phase field parameter that varies from 0 (solid) to 1 (liquid) and defines the freezing front. Parameters such as surface tension and interface kinetic coefficients are included into the model in order to capture physics of the problem. In addition, conditions for nucleation are considered and modeled. This study provides a better understanding of how supercooling impacts biological cells and tissues and how to avoid the damage of them. In [6], an optimal control problem for a phase field model is stated and investigated both from mathematical and algorithmical points of view. The design of optimal controls utilizes gradient descent methods and techniques of adjoint equations. Optimized cooling protocols for the reduction of damaging effects caused by the latent heat release and delayed freezing of the intracellular liquid are designed in [7] on the basis of results of [4,6,8]. A model of freezing of liquids in porous media from [8] is used to describe ice formation in the extracellular matrix.

It should be mentioned, however, that the spatial distribution of parameters is not very important, if small objects such as living cells are investigated. By integrating of partial differential equations over appropriate domains, one can average spatially distributed models and reduce them to several ordinary differential equations with control parameters and uncertainties. Such averaging techniques go back to the heat balance integral method of Goodman see [9,10]. The averaged approximate equations contain very often nonlinear dependencies given by tabular data. Thus, the uncertainties and non-smooth nonlinearities complicate the application of traditional control design methods based on Pontryagin’s maximum principle. Nevertheless, the dynamical programming principle related to Hamilton–Jacobi–Bellman–Isaacs (HJBI) equations is suitable. The application of this technique requires stable grid methods for solving HJBI equations arising from the above mentioned problems. This paper considers a stable grid procedure that allows us to design optimized controls (cooling protocols) in a model describing competitive ice formation inside and outside of a living cell.

2. Mathematical model of ice formation

Cryopreservation of living cells is a necessary part of many medical procedures. However, cells and tissues can be damaged by the cryopreservation process itself. One of injuring factors of cryopreservation is mechanical damage of cells caused by the volume increase during the water to ice phase change. The cells of a tissue are surrounded by an extracellular liquid confined in small vessels of an extracellular matrix. Biologists suppose that cells may communicate through these vessels. However, the mechanism and the role of cell–cell interactions are still not well understood see e.g. [11]. We will consider a simplified model which does not take into account possible cell–cell interactions. For this reason, the extracellular liquid is assumed to be confined in small non-communicating cavities or pores of the extracellular matrix. Each cell has a membrane that provides a physical separation between the intra- and extracellular environments, which may cause delayed freezing of the intracellular liquid. This effect results in a very large stress exerted on the cell membrane. To avoid that, the liquids inside and outside the cell must freeze simultaneously. This can be achieved through lowering the freezing point of the extracellular fluid and optimization of cooling protocols.

Fig. 1 sketches an extracellular matrix with pores containing living cells. The extracellular fluid freezes earlier than the intracellular one, and the volumetric increase of ice produces a great pressure exerted on cells. The magnitude of the effect can be approximately estimated as

$$p \approx \text{tr}(C^{ice})\alpha \cdot (1 - \beta_\ell),$$

where p is the pressure exerted on the cell membrane, C^{ice} is the elastic tensor of ice, α is the ratio of volume expansion due to the water-to-ice phase transition, β_ℓ is the unfrozen water content so that $1 - \beta_\ell$ is the ice content.

The unfrozen water content, β_ℓ , in a cell or in the extracellular space can be computed using the following phase field model see [8]:

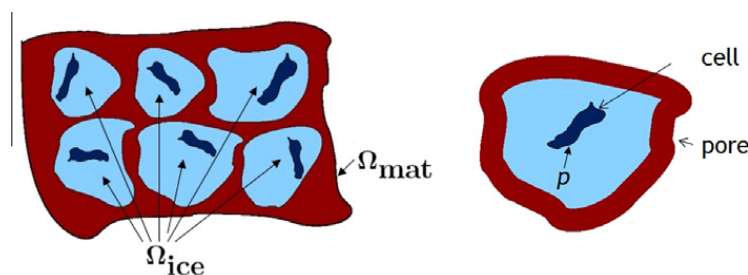


Fig. 1. Two-dimensional sketch of the extracellular matrix with pores containing living cells.

$$\beta_\ell(\theta) = \phi \left(\frac{L(\theta - \theta_s)}{(T_0 + \theta_s)(T_0 + \theta)} \right), \quad e(\theta) = \rho C \theta + \rho L \beta_\ell(\theta), \quad (1)$$

$$\frac{\partial e(\theta)}{\partial t} - \mathcal{K} \Delta \theta = 0, \quad -\mathcal{K} \frac{\partial \theta}{\partial \nu} \Big|_{\partial \Omega} = \lambda(\theta - \theta_E) \Big|_{\partial \Omega},$$

where $\Omega \subset R^3$ is either intra- or extracellular space, θ the Celsius temperature, θ_s the freezing (solidification) point, T_0 the Celsius zero point (273 K), ρ the density, C the specific heat capacity, L the specific latent heat, \mathcal{K} the heat conductivity coefficient. The function $e(\theta)$ has the sense of the internal energy. The function ϕ is recovered from data obtained in experiments with tissue samples. A typical form of the function $\beta_\ell(\theta)$ is shown in Fig. 2.

To obtain a model based on ordinary differential equations, integrate the phase field model (1) over the regions shown in Fig. 3. The notation is as follows: Ω_2 is the region occupied by the cell; Ω_1 is the extracellular region; Γ_2 represents the cell membrane; Γ_1 is the boundary of the extracellular space; θ_2, θ_1 , and θ_E are the temperatures in the cell, extracellular space, and outside of the pore, respectively; e_2 and e_1 are the internal energies in the cell and extracellular space, respectively; and θ_{2s}, θ_{1s} are the corresponding freezing temperatures.

Integrating the energy balance equation of (1) over Ω_1 and assuming the film heat transfer condition for the pore boundary, Γ_1 , and the cell membrane, Γ_2 , yield

$$\frac{d}{dt} \int_{\Omega_1} e_1 dV + \lambda \int_{\Gamma_1} (\theta_1 - \theta_E) dS + \alpha \int_{\Gamma_2} (\theta_1 - \theta_2) dS = 0,$$

where λ and α are the corresponding film thermal conductivity coefficients. Analogously, integrating over Ω_2 gives

$$\frac{d}{dt} \int_{\Omega_2} e_2 dV + \alpha \int_{\Gamma_2} (\theta_2 - \theta_1) dS = 0.$$

With the notation

$$\hat{e}_i = \frac{1}{|\Omega_i|} \int_{\Omega_i} e_i dV, \quad \hat{\theta}_i = \frac{1}{|\Gamma_i|} \int_{\Gamma_i} \theta_i dS, \quad \hat{\theta}_E = \frac{1}{|\Gamma_1|} \int_{\Gamma_1} \theta_E dS,$$

$$\hat{\alpha}_i = \frac{|\Gamma_2|}{|\Omega_i|} \alpha, \quad \hat{\lambda} = \frac{|\Gamma_1|}{|\Omega_1|} \lambda$$

for the mean values and the assumption that $|\Gamma_1|^{-1} \int_{\Gamma_1} \theta_1 dS \approx |\Gamma_2|^{-1} \int_{\Gamma_2} \theta_1 dS$ because θ_1 is almost constant in the small region Ω_1 , we arrive at the coupled system of ordinary differential equations

$$\begin{aligned} \frac{d}{dt} \hat{e}_1 &= -\hat{\alpha}_1 [\hat{\theta}_1 - \hat{\theta}_2] - \hat{\lambda} [\hat{\theta}_1 - \hat{\theta}_E], \\ \frac{d}{dt} \hat{e}_2 &= -\hat{\alpha}_2 [\hat{\theta}_2 - \hat{\theta}_1]. \end{aligned} \quad (2)$$

Here, the relation between \hat{e}_i and $\hat{\theta}_i$ is given by the formula (see (1)):

$$\hat{e}_i = \rho C \hat{\theta}_i + \rho L \beta_\ell^i(\hat{\theta}_i). \quad (3)$$

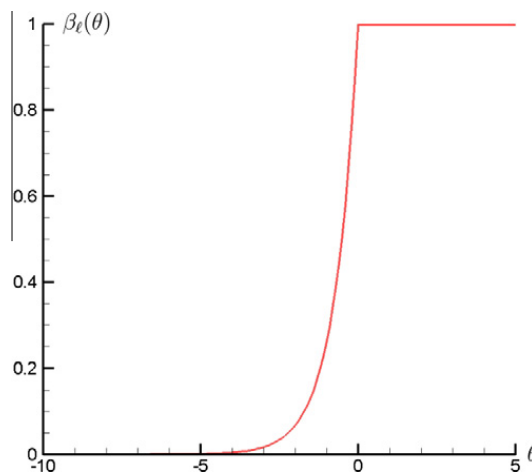


Fig. 2. Dependence of the extracellular water content on the temperature.

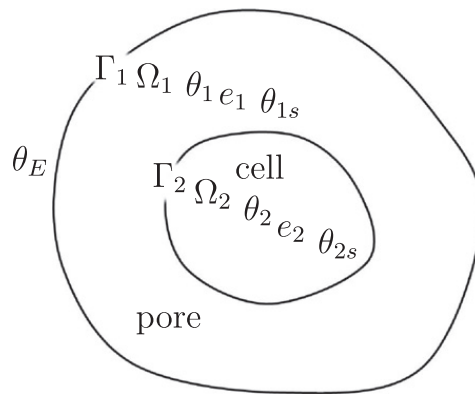


Fig. 3. Schematic notation of variables and three-dimensional regions when considering a single pore. Note that Γ_1 and Γ_2 are the boundaries of the pore and the cell, respectively, Ω_1 is the region lying between Γ_1 and Γ_2 (extracellular space), and Ω_2 is the region of the cell.

Note that the derivatives $\partial \hat{e}_i / \partial \hat{\theta}_i$, $i = 1, 2$, are discontinuous (see Fig. 4). Therefore, the direct form of Eq. (2) is not appropriate. It is convenient to express the temperatures $\hat{\theta}_1$ and $\hat{\theta}_2$ through the energies \hat{e}_1 and \hat{e}_2 , respectively, using the relation $\hat{\theta}_i = \Theta_i(\hat{e}_i)$ which is the inverse of relation (3), see Fig. 5. Such techniques are closely related to the standard enthalpy method see e.g. [10]. By doing that, we obtain the following system of differential equations:

$$\begin{aligned} \dot{\hat{e}}_1 &= -\hat{\alpha}_1[\Theta_1(\hat{e}_1) - \Theta_2(\hat{e}_2)] - \hat{\lambda}[\Theta_1(\hat{e}_1) - \hat{\theta}_E] \\ \dot{\hat{e}}_2 &= -\hat{\alpha}_2[\Theta_2(\hat{e}_2) - \Theta_1(\hat{e}_1)]. \end{aligned} \tag{4}$$

For simplicity, denote $x = \hat{e}_1$, $y = \hat{e}_2$, $z = \hat{\theta}_E$, $\alpha_1 = \hat{\alpha}_1$, $\lambda = \hat{\lambda}$ and consider the following controlled system

$$\begin{aligned} \dot{x} &= -\alpha_1[\Theta_1(x) - \Theta_2(y)] - \lambda[\Theta_1(x) - z] - d + v_1 \\ \dot{y} &= -\alpha_2[\Theta_2(y) - \Theta_1(x)] + v_2 \\ \dot{z} &= u. \end{aligned} \tag{5}$$

Here, z is the temperature outside of the pore (the chamber temperature), u is the cooling rate, v_1 , v_2 are errors in data interpreted as disturbances. The control u is restricted by the relation $-\mu \leq u \leq 0$ (μ is positive). The disturbances v_1 and v_2 are bounded as follows: $|v_1| \leq v$, $|v_2| \leq v$. Since the zero initial value for z is always assumed, a constant d is introduced to emulate nonzero initial values of z (the initial chamber temperature).

According to the meaning of the functions β_i^i , $i = 1, 2$, exact simultaneous freezing of the extracellular and intracellular liquids can be expressed as the vanishing of one of the following functionals:

$$J_1 = \int_0^{t_f} \gamma^2(x(t), y(t)) dt, \tag{6}$$

$$J_2 = \max_{t \in [0, t_f]} \gamma(x(t), y(t)), \tag{7}$$

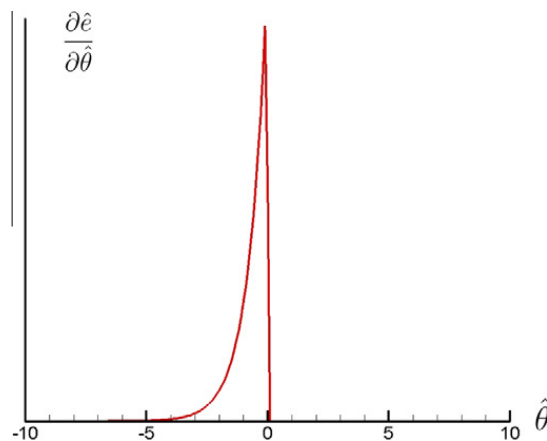


Fig. 4. Graph of the function $\frac{\partial \hat{e}}{\partial \hat{\theta}}$, see formula (3) and Fig. 2.

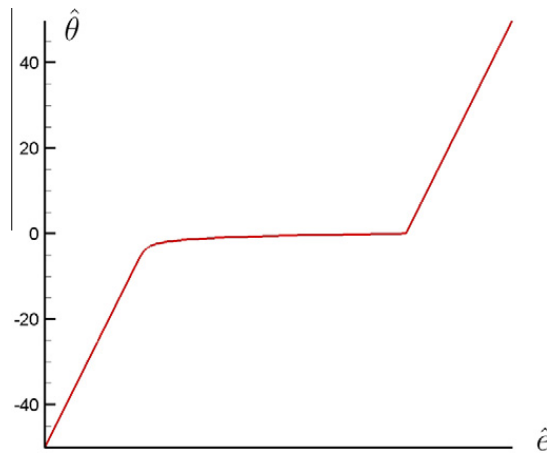


Fig. 5. Graph of the inverse function of $\hat{\theta}(\hat{e})$.

where the function

$$\gamma(x, y) := |\beta_\ell^1(\Theta_1(x)) - \beta_\ell^2(\Theta_2(y))|,$$

estimates the difference of the ice content in the intra- and extracellular regions.

Note that the functional (6) simultaneously estimates the amount of liquid flowing out from the cell. In fact, let W_{in}^0, W_{in} be the initial and current volume of the intracellular liquid, respectively, and W_{out}^0, W_{out} are the same but for the extracellular liquid. Denote by c_{in}^0 and c_{in} the initial and current salt concentrations in the intracellular liquid. Similarly, c_{out}^0 and c_{out} are the initial and current salt concentrations in the extracellular liquid. Observing that

$$W_{in}(t) \approx W_{in}^0 \beta_\ell^2(\Theta_2(y(t))), \quad W_{out}(t) \approx W_{out}^0 \beta_\ell^1(\Theta_1(x(t)))$$

and using the mass conservation law yield the following relations:

$$c_{in}(t) = \frac{c_{in}^0 W_{in}^0}{W_{in}(t)}, \quad c_{out}(t) = \frac{c_{out}^0 W_{out}^0}{W_{out}(t)}.$$

Therefore,

$$|c_{in}(t) - c_{out}(t)| = \left| \frac{c_{in}^0}{\beta_\ell^2(\Theta_2(y(t)))} - \frac{c_{out}^0}{\beta_\ell^1(\Theta_1(x(t)))} \right|.$$

Multiplying both parts of the last relation by the factor $\beta_\ell^1 \beta_\ell^2$ which evaluates the free-of-ice part of the cell membrane and assuming that $c_{in}^0 = c_{out}^0$ give

$$|c_{in}(t) - c_{out}(t)| \beta_\ell^1 \beta_\ell^2 = c_{in}^0 |\beta_\ell^1(\Theta_1(x(t))) - \beta_\ell^2(\Theta_2(y(t)))|.$$

Therefore, the minimization of the functional (6) or (7) contributes to the reduction of cell dehydration.

Consider differential game (5) and (6) (resp. (5) and (7)) where the objective of the control u is to minimize the functional J_1 (resp. J_2), whereas the objective of the disturbance is opposite. The differential game will be solved numerically using approximation scheme described in Section 5. The value function [23] will be computed as a viscosity solution to the corresponding HJBI equation, and the optimal feedback control will be found by applying the extremal aiming procedure, see [12–14].

The next section outlines the setting of differential game theory and its connection to HJBI equations.

3. Differential games and Hamilton–Jacobi–Bellman–Isaacs equations

Consider the following differential game

$$\dot{x} = f(t, x, u, v), \tag{8}$$

where $x \in R^n$ is the state vector, u and v are control parameters of the first and second players, respectively, restricted by the relations

$$u \in P \subset R^p, \quad v \in Q \subset R^q. \tag{9}$$

Here, P and Q are given compacts. The game starts at $t_0 \in [0, t_f]$ and finishes at t_f . Two types of payoff functionals will be considered. The first one being of the form

$$J_1(x(\cdot)) = \int_{t_0}^{t_f} \sigma(t, x(t)) dt \tag{10}$$

and the second one is given by

$$J_2(x(\cdot)) = \max \text{ (or) } \min_{t \in [t_0, t_f]} \sigma(t, x(t)), \tag{11}$$

where $\sigma : [0, t_f] \times R^n \rightarrow R$ is some given function. The objective of the control u of the first player is to minimize the functional (10) (resp. (11)), whereas the objective of the control v of the second player is opposite.

Assume that the following conditions are fulfilled:

- (f1) The function f is uniformly continuous on $[0, t_f] \times R^n \times P \times Q$.
- (f2) f is bounded, i.e.

$$|f(t, x, u, v)| \leq M$$

for all $(t, x, u, v) \in [0, t_f] \times R^n \times P \times Q$.

- (f3) f is Lipschitz-continuous in t, x , i.e.

$$|f(t_1, x_1, u, v) - f(t_2, x_2, u, v)| \leq N(|t_1 - t_2| + |x_1 - x_2|)$$

for all $(t_i, x_i, u, v) \in [0, t_f] \times R^n \times P \times Q, i = 1, 2$.

- (f4) σ is bounded and Lipschitz-continuous in t, x , i.e.

$$|\sigma(t, x)| \leq C_0$$

and

$$|\sigma(t_1, x_1) - \sigma(t_2, x_2)| \leq L_0(|t_1 - t_2| + |x_1 - x_2|)$$

for all $(t, x), (t_i, x_i) \in [0, t_f] \times R^n, i = 1, 2$.

- (f5) f satisfies the saddle point condition, i.e.

$$\min_{u \in P} \max_{v \in Q} \langle \ell, f(t, x, u, v) \rangle = \max_{v \in Q} \min_{u \in P} \langle \ell, f(t, x, u, v) \rangle$$

for any $\ell \in R^n, (t, x) \in [0, t_f] \times R^n$.

- (f5a) $f(t, x, u, v) = g_1(t, x, u) + g_2(t, x, v)$, where g_1 (resp. g_2) is linear in u (resp. in v) for each fixed t and x . Obviously, (f5a) implies (f5).

The game (8)–(11) is formalized as in [12–15]. The players use feedback strategies which are arbitrary functions

$$\mathcal{P} : [0, t_f] \times R^n \rightarrow P, \quad \mathcal{Q} : [0, t_f] \times R^n \rightarrow Q.$$

For any initial position $(t_0, x_0) \in [0, t_f] \times R^n$ and any strategies \mathcal{P} and \mathcal{Q} , two functional sets $X_1(t_0, x_0, \mathcal{P})$ and $X_2(t_0, x_0, \mathcal{Q})$ are defined. These sets consist of limits of the step-by-step solutions of (8) generated by the strategies \mathcal{P} and \mathcal{Q} , respectively, see [12–15].

It is well-known due to [13–15] that, under assumptions (f1)–(f5), the differential game (8)–(10) (resp. (8), (9) and (11)) has a value function $V : (t, x) \rightarrow V(t, x)$ defined by the relation

$$V(t, x) = \min_P \max_{x(\cdot) \in X_1(t, x, P)} J(x(\cdot)) = \max_Q \min_{x(\cdot) \in X_2(t, x, Q)} J(x(\cdot)),$$

where $J = J_1$ (resp. J_2). The value function is bounded and Lipschitz-continuous in t, x .

The next important result proved in [16] says that the value function V coincides with the viscosity solution see [17–19] of the following HJBI equation:

$$V_t + H(t, x, V_x) = 0, \tag{12}$$

where the Hamiltonian H and the terminal condition are defined as

$$H(t, x, p) = \max_{v \in Q} \min_{u \in P} \langle p, f(t, x, u, v) \rangle + \sigma(t, x), \quad V(t_f, x) = 0$$

in the case of the payoff functional (10). In the case of the payoff functional (11), the Hamiltonian and the terminal condition are of the form

$$H(t, x, p) = \max_{v \in Q} \min_{u \in P} \langle p, f(t, x, u, v) \rangle, \quad V(t_f, x) = \sigma(t_f, x)$$

and the viscosity solution is defined in a special way see [20].

In the next section, approximation schemes for solving Eq. (12) are discussed and convergence results are given.

4. Approximation schemes and convergence results

The consideration of this section will be carried out in R^3 so that the state variables are $x, y,$ and z . Moreover, the time-independence of the right-hand-side of the controlled system and the function σ is assumed for brevity. However, all results are valid for arbitrary space dimensions and time dependent systems.

In [20], a finite difference scheme for finding viscosity solutions to Eq. (12) with the payoff functional of the form (10) or (11) has been proposed. The scheme is based on a solution operator which can be considered as a modification of the abstract solution operator introduced in [21]. Similarly to [21], the convergence result has been proved under requirement of the monotonicity property of the solution operator. The present paper describes (see Section 5) a monotone finite difference scheme based on a solution operator introduced in [22]. The main idea of obtaining the monotonicity is to use either the right or the left divided differences for the approximation of the spatial derivatives $V_x, V_y,$ and V_z depending on the sign of $f_1, f_2,$ and $f_3,$ respectively. Here, f_i denotes the i th component of the right hand side of the controlled system.

Let $\Delta_x, \Delta_y, \Delta_z,$ and τ are spatial and time discretization steps, respectively. Introduce the notation

$$V^n(x_i, y_j, z_k) = V(n\tau, i\Delta_x, j\Delta_y, k\Delta_z), \quad n = 0, \dots, N := t_f/\tau$$

and consider a difference scheme

$$V^{n-1}(x_i, y_j, z_k) = V^n(x_i, y_j, z_k) + \tau H(x_i, y_j, z_k, V_x^n, V_y^n, V_z^n),$$

where

$$V^N(x_i, y_j, z_k) = 0 \text{ or } V^N(x_i, y_j, z_k) = \sigma(x_i, y_j, z_k),$$

depending on the choice of the payoff functional (J_1 or J_2). The symbols V_x^n, V_y^n, V_z^n denote finite difference approximations (left, right, central and etc.) of the corresponding partial derivatives.

The scheme can be considered as the successive application of an operator Π to grid functions so that

$$V^{n-1} = \Pi(V^n; \tau, \Delta_x, \Delta_y, \Delta_z).$$

Note that such an operator can be naturally extended to continuum functions.

Definition 1. The operator Π is monotone, if the following implication holds:

$$V \leq W \Rightarrow \Pi(V; \tau, \Delta_x, \Delta_y, \Delta_z) \leq \Pi(W; \tau, \Delta_x, \Delta_y, \Delta_z),$$

where the point-wise order is assumed.

Definition 2. The operator Π has the generator property, if the following estimate holds:

$$\left| \frac{\Pi(\phi; \tau, a\tau, b\tau, c\tau)(\vec{r}) - \phi(\vec{r})}{\tau} - H(\vec{r}, D\phi(\vec{r})) \right| \leq C(1 + \|D\phi\| + \|D^2\phi\|)\tau \tag{13}$$

for every $\phi \in C_b^2(R^3), \vec{r} = (x, y, z) \in R^3,$ and fixed $a, b, c > 0.$

Here $C_b^2(R^3)$ is the space of twice continuously differentiable functions defined on R^3 and bounded together with their two derivatives, $\|\cdot\|$ denotes the point-wise maximum norm, $D\phi$ and $D^2\phi$ denote the gradient and the Hessian matrix of $\phi.$

Theorem 1 (Convergence, [21]). Assume that the operator $\Pi(\cdot; \tau, a\tau, b\tau, c\tau)$ is monotone for any $\tau > 0$ and satisfies the generator property, then the grid function obtained by the procedure:

$$V^{n-1} = \Pi(V^n; \tau, a\tau, b\tau, c\tau), \quad V^N = 0,$$

converges point-wise to the value function of the differential game (8)–(10) as $\tau \rightarrow 0,$ and the convergence rate is $\sqrt{\tau}.$

Theorem 2 (Convergence, [20]). Assume that the operator $\Pi(\cdot; \tau, a\tau, b\tau, c\tau)$ is monotone for any $\tau > 0$ and satisfies the generator property, then the grid function obtained by the procedure:

$$V^{n-1} = \max \text{ (or) } \min \{ \Pi(V^n; \tau, a\tau, b\tau, c\tau), \sigma \}, \quad V^N = \sigma,$$

converges point-wise to the value function of the differential game (8), (9) and (11) as $\tau \rightarrow 0,$ and the convergence rate is $\sqrt{\tau}.$

Remark 1. Theorems 1 and 2 refer only to the monotonicity and generator properties of the operator $\Pi.$ Actually, some secondary properties have to hold in order to claim the convergence see [21,20]. We omit here the discussion of them because they obviously hold for the operator Π considered below.

The next section describes an operator Π possessing the monotonicity property.

5. Upwind solution operator

Let us investigate a solution operator proposed in [22]. We will prove that this operator is monotone under a certain relation between $\Delta_x, \Delta_y, \Delta_z$, and τ . Unfortunately, the convergence arguments given in [22] are very sketchy and not strong. They are solely based on topological considerations and do not take into account the nature of viscosity solutions. Nevertheless, the idea of the operator proposed is valuable. Denote

$$a^+ = \max(a, 0), \quad a^- = \min(a, 0).$$

The operator introduced in [22] assumes the following approximations of the spatial derivatives:

$$V_x^n \cdot f_1 := p_1^R \cdot f_1^+ + p_1^L \cdot f_1^-, \quad V_y^n \cdot f_2 := p_2^R \cdot f_2^+ + p_2^L \cdot f_2^-, \quad V_z^n \cdot f_3 := p_3^R \cdot f_3^+ + p_3^L \cdot f_3^-,$$

where f_1, f_2, f_3 are the right hand sides of the controlled system computed at (x_i, y_j, z_k) , p_1^R, p_2^R, p_3^R and p_1^L, p_2^L, p_3^L the right and the left divided differences, respectively, defined by

$$p_1^R = [V^n(x_{i+1}, y_j, z_k) - V^n(x_i, y_j, z_k)]/\Delta_x,$$

$$p_2^R = [V^n(x_i, y_{j+1}, z_k) - V^n(x_i, y_j, z_k)]/\Delta_y,$$

$$p_3^R = [V^n(x_i, y_j, z_{k+1}) - V^n(x_i, y_j, z_k)]/\Delta_z,$$

$$p_1^L = [V^n(x_i, y_j, z_k) - V^n(x_{i-1}, y_j, z_k)]/\Delta_x,$$

$$p_2^L = [V^n(x_i, y_j, z_k) - V^n(x_i, y_{j-1}, z_k)]/\Delta_y,$$

$$p_3^L = [V^n(x_i, y_j, z_k) - V^n(x_i, y_j, z_{k-1})]/\Delta_z.$$

Finally, the operator is given by

$$\begin{aligned} \Pi(V^n; \tau, \Delta_x, \Delta_y, \Delta_z)(x_i, y_j, z_k) &= V^n(x_i, y_j, z_k) + \tau \max_{v \in Q} \min_{u \in P} (p_1^R \cdot f_1^+ + p_1^L \cdot f_1^- + p_2^R \cdot f_2^+ + p_2^L \cdot f_2^- + p_3^R \cdot f_3^+ + p_3^L \cdot f_3^-) \\ &\quad + \tau \sigma(x_i, y_j, z_k) \end{aligned} \tag{14}$$

in the case of functional J_1 (without σ if J_2).

Lemma 1 (Monotonicity). *Let M be the bound of the right hand side of the controlled system. If $a, b, c \geq M\sqrt{3}$, then the operator $\Pi(\cdot; \tau, a\tau, b\tau, c\tau)$ given by (14) is monotone.*

Proof. Suppose $V \leq W$. Let us show that $\Pi(V; \tau, a\tau, b\tau, c\tau) \leq \Pi(W; \tau, a\tau, b\tau, c\tau)$.

We have

$$\begin{aligned} &\Pi(V; \tau, a\tau, b\tau, c\tau)(x, y, z) - \Pi(W; \tau, a\tau, b\tau, c\tau)(x, y, z) \\ &= V(x, y, z) - W(x, y, z) + \tau \left[\max_{v \in Q} \min_{u \in P} \left(\frac{V(x + a\tau, y, z) - V(x, y, z)}{a\tau} \cdot f_1^+ + \frac{V(x, y + b\tau, z) - V(x, y, z)}{b\tau} \cdot f_2^+ \right. \right. \\ &\quad + \frac{V(x, y, z + c\tau) - V(x, y, z)}{c\tau} \cdot f_3^+ + \frac{V(x, y, z) - V(x - a\tau, y, z)}{a\tau} \cdot f_1^- + \frac{V(x, y, z) - V(x, y - b\tau, z)}{b\tau} \cdot f_2^- \\ &\quad + \left. \frac{V(x, y, z) - V(x, y, z - c\tau)}{c\tau} \cdot f_3^- \right) - \max_{v \in Q} \min_{u \in P} \left(\frac{W(x + a\tau, y, z) - W(x, y, z)}{a\tau} \cdot f_1^+ + \frac{W(x, y + b\tau, z) - W(x, y, z)}{b\tau} \cdot f_2^+ \right. \\ &\quad + \frac{W(x, y, z + c\tau) - W(x, y, z)}{c\tau} \cdot f_3^+ + \frac{W(x, y, z) - W(x - a\tau, y, z)}{a\tau} \cdot f_1^- + \frac{W(x, y, z) - W(x, y - b\tau, z)}{b\tau} \cdot f_2^- \\ &\quad + \left. \frac{W(x, y, z) - W(x, y, z - c\tau)}{c\tau} \cdot f_3^- \right) \Big]. \end{aligned}$$

By rearranging terms and using the obvious relations $f^+ - f^- = |f|$ and $\min_u g_1(u) - \min_u g_2(u) \leq \max_u [g_1(u) - g_2(u)]$, one obtains

$$\begin{aligned} \Pi(V; \tau, a\tau, b\tau, c\tau)(x, y, z) - \Pi(W; \tau, a\tau, b\tau, c\tau)(x, y, z) &\leq V(x, y, z) - W(x, y, z) \\ &\quad - \tau \left(\frac{|f_1|}{a\tau} + \frac{|f_2|}{b\tau} + \frac{|f_3|}{c\tau} \right) (V(x, y, z) - W(x, y, z)) = \left[1 - \left(\frac{|f_1|}{a} + \frac{|f_2|}{b} + \frac{|f_3|}{c} \right) \right] (V(x, y, z) - W(x, y, z)). \end{aligned}$$

With $|f_1| + |f_2| + |f_3| \leq \sqrt{3}M$ (in the case of n variables the relation $\sum_{i=1}^n |f_i| \leq \sqrt{n \sum_{i=1}^n f_i^2}$ is applied) we obtain $\left[1 - \left(\frac{|f_1|}{a} + \frac{|f_2|}{b} + \frac{|f_3|}{c} \right) \right] \geq 0$, which finally implies the required inequality. \square

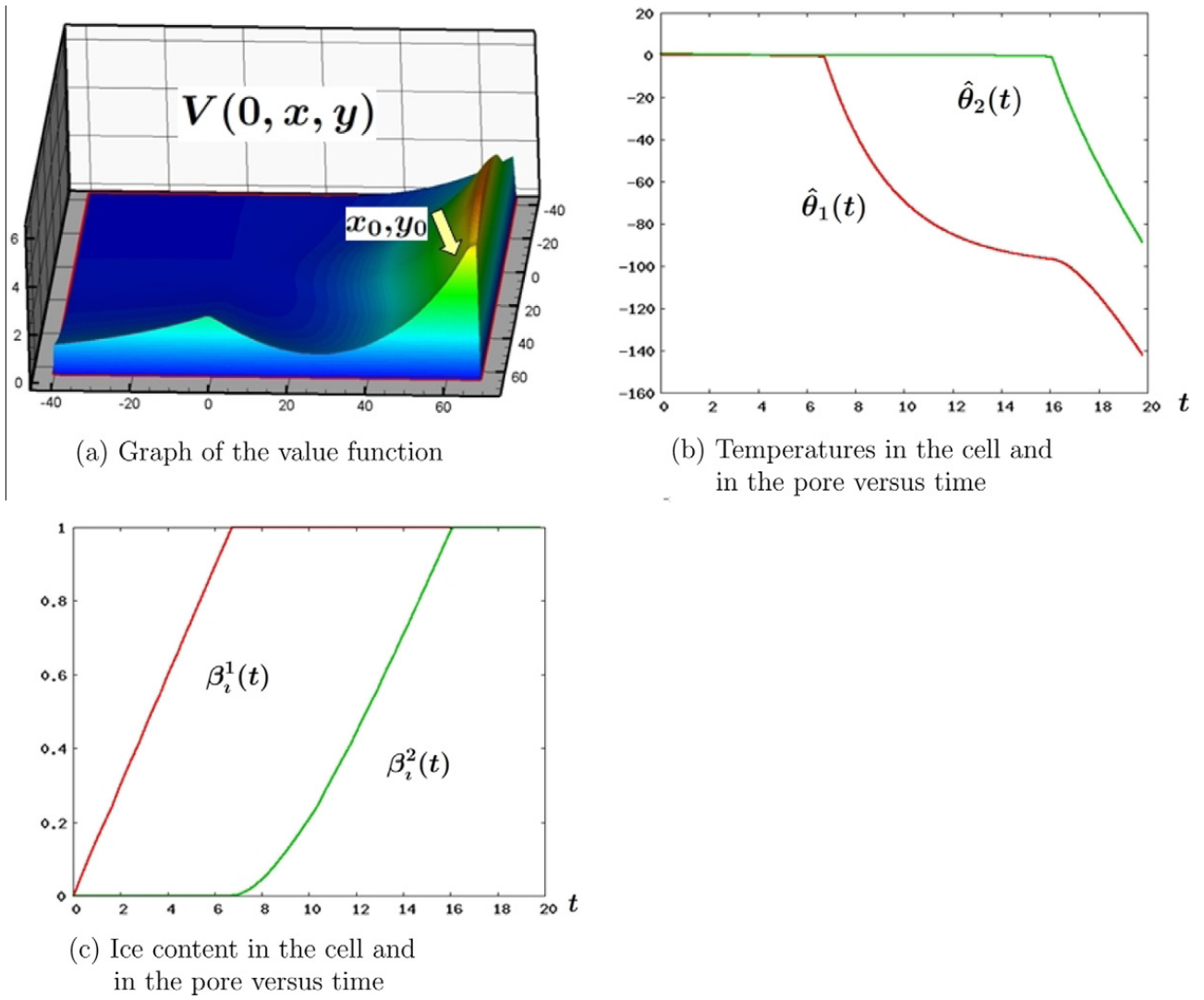


Fig. 6. The case of infinite cooling rate and functional J_1 . Here $\theta_{1s} = \theta_{2s}$.

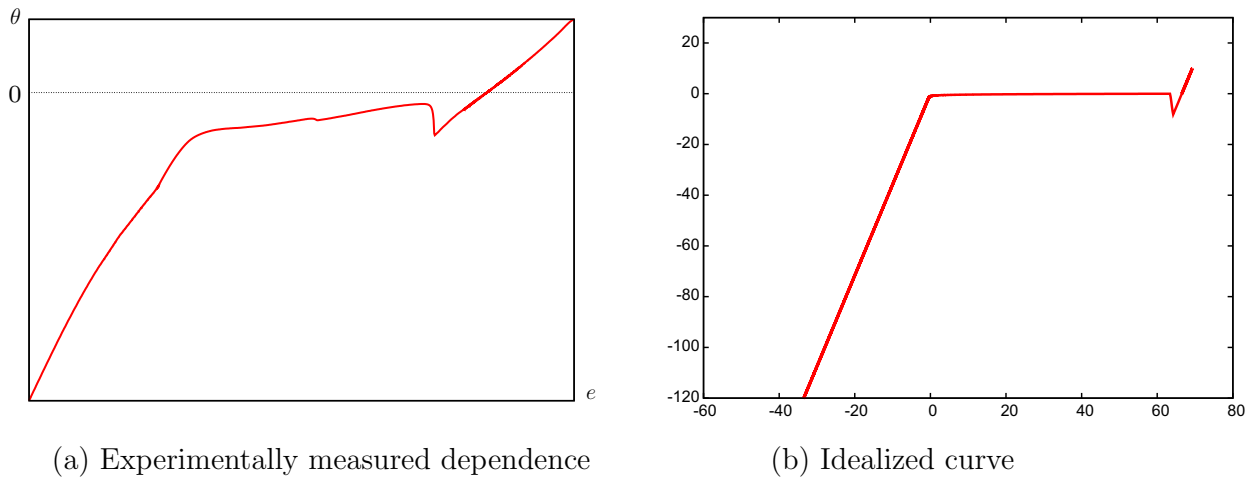
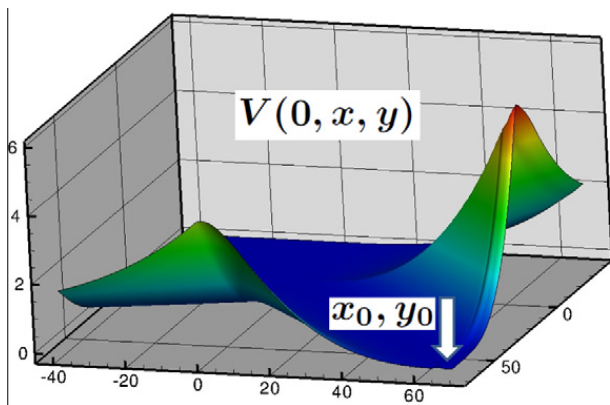
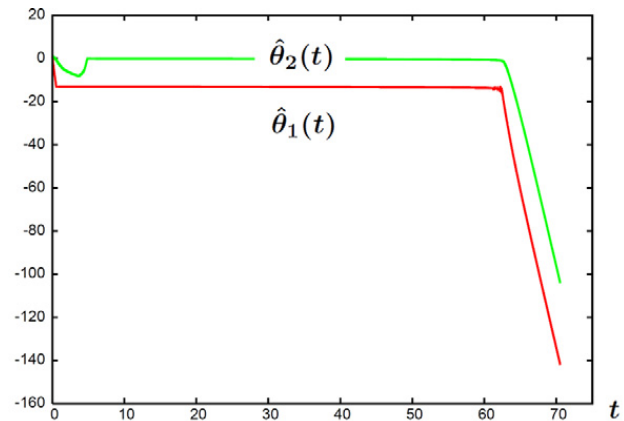


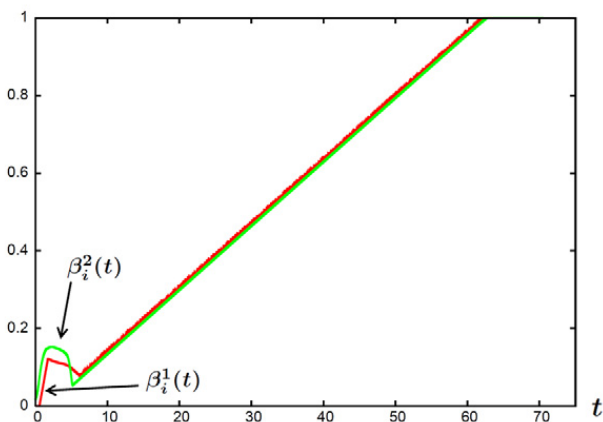
Fig. 7. Supercooling effect in the intracellular liquid displays itself as a kink in the dependence of the temperature on the internal energy.



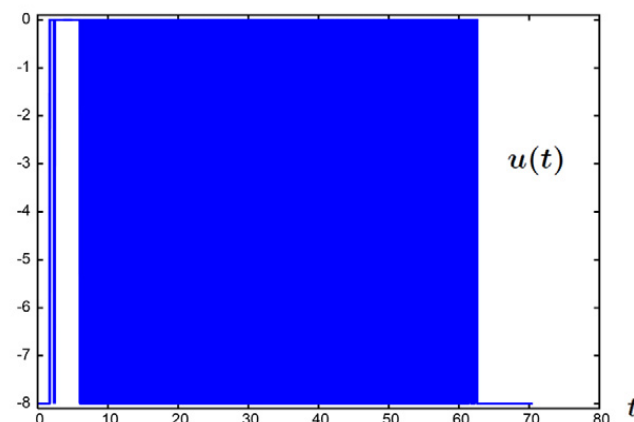
(a) Graph of the value function



(b) Temperatures in the cell and in the pore versus time



(c) Ice content in the cell and in the pore versus time



(d) Realization of the control with extremely frequent switches

Fig. 8. The case of infinite cooling rate and functional J_1 . Here $\theta_{1s} - \theta_{2s} = -13^\circ\text{C}$.

Lemma 2 (Generator property). *The generator property (13) holds.*

Proof. Consider the case of functional J_1 (the proof for the functional J_2 is obtained by letting $\sigma = 0$).

Let $\phi \in C_b^2(\mathbb{R}^3)$ and $(x, y, z) \in \mathbb{R}^3$. We have

$$\begin{aligned} \Pi(\phi; \tau, \Delta_x, \Delta_y, \Delta_z)(x, y, z) = & \phi(x, y, z) + \tau \max_{v \in Q} \min_{u \in P} \left[\frac{\phi(x + \Delta_x, y, z) - \phi(x, y, z)}{\Delta_x} \cdot f_1^+ + \frac{\phi(x, y, z) - \phi(x - \Delta_x, y, z)}{\Delta_x} \cdot f_1^- \right. \\ & + \frac{\phi(x, y + \Delta_y, z) - \phi(x, y, z)}{\Delta_y} \cdot f_2^+ + \frac{\phi(x, y, z) - \phi(x, y - \Delta_y, z)}{\Delta_y} \cdot f_2^- + \frac{\phi(x, y, z + \Delta_z) - \phi(x, y, z)}{\Delta_z} \cdot f_3^+ \\ & \left. + \frac{\phi(x, y, z) - \phi(x, y, z - \Delta_z)}{\Delta_z} \cdot f_3^- \right] + \tau \sigma(x, y, z). \end{aligned}$$

Remember $f = (f_1, f_2, f_3)$ is the right-hand side of the controlled system. Estimate

$$\begin{aligned} & \left| \frac{\Pi(\phi; \tau, \Delta_x, \Delta_y, \Delta_z)(x, y, z) - \phi(x, y, z)}{\tau} - \max_{v \in Q} \min_{u \in P} \langle D\phi(x, y, z), f \rangle - \sigma(x, y, z) \right| \\ & \leq \max_{u \in P} \max_{v \in Q} \left| \left(\frac{\phi(x + \Delta_x, y, z) - \phi(x, y, z)}{\Delta_x} - \frac{\partial \phi}{\partial x}(x, y, z) \right) \cdot f_1^+ + \left(\frac{\phi(x, y + \Delta_y, z) - \phi(x, y, z)}{\Delta_y} - \frac{\partial \phi}{\partial y}(x, y, z) \right) \cdot f_2^+ \right. \\ & \quad + \left(\frac{\phi(x, y, z + \Delta_z) - \phi(x, y, z)}{\Delta_z} - \frac{\partial \phi}{\partial z}(x, y, z) \right) \cdot f_3^+ + \left(\frac{\phi(x, y, z) - \phi(x - \Delta_x, y, z)}{\Delta_x} - \frac{\partial \phi}{\partial x}(x, y, z) \right) \cdot f_1^- \\ & \quad + \left(\frac{\phi(x, y, z) - \phi(x, y - \Delta_y, z)}{\Delta_y} - \frac{\partial \phi}{\partial y}(x, y, z) \right) \cdot f_2^- + \left. \left(\frac{\phi(x, y, z) - \phi(x, y, z - \Delta_z)}{\Delta_z} - \frac{\partial \phi}{\partial z}(x, y, z) \right) \cdot f_3^- \right| \\ & \leq M \cdot \|D^2 \phi\| (\Delta_x + \Delta_y + \Delta_z). \end{aligned}$$

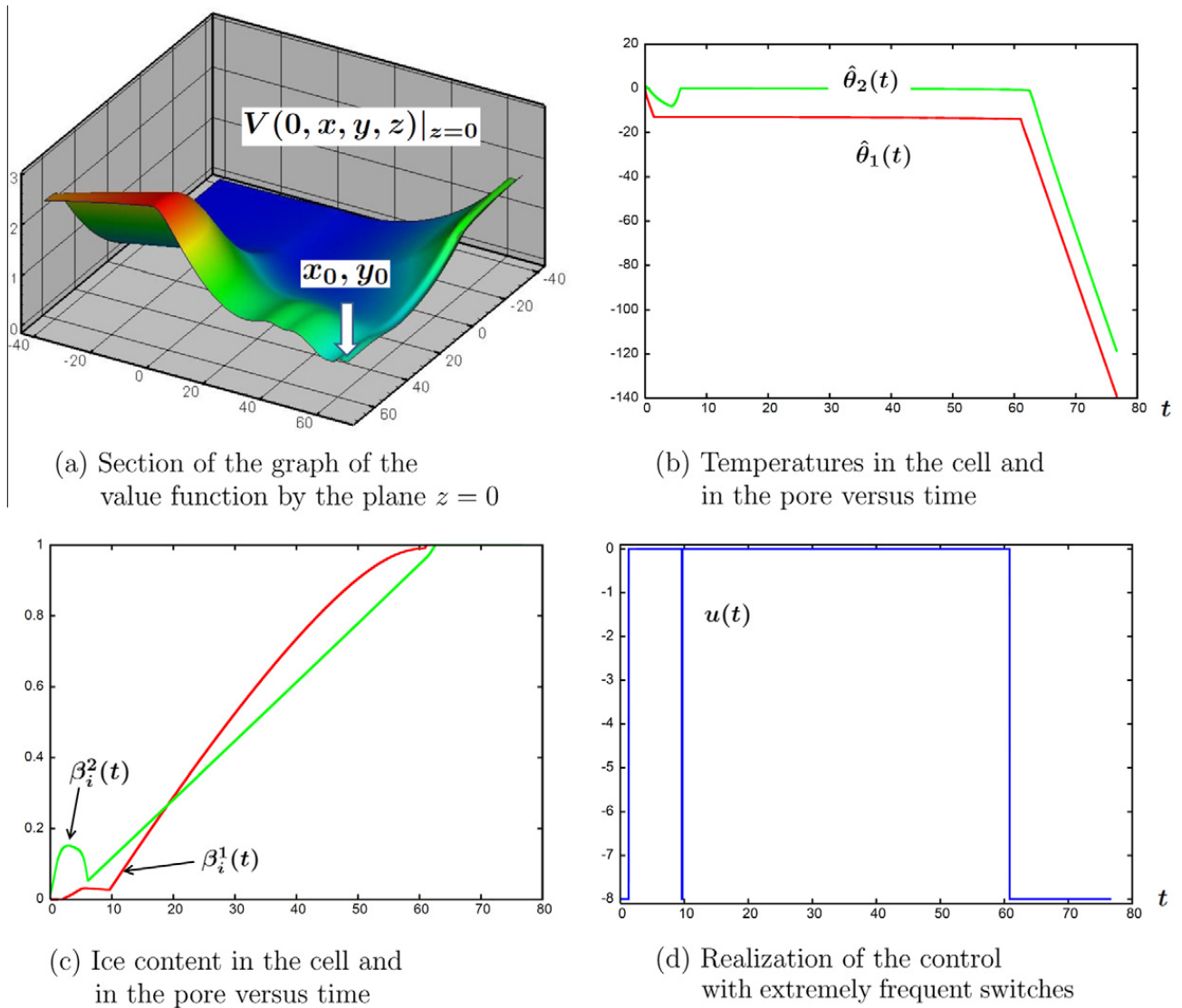


Fig. 9. The case of finite cooling rate and functional J_1 . Here $\theta_{1s} - \theta_{2s} = -13^\circ\text{C}$.

Choosing $\Delta_x = a\tau$, $\Delta_y = b\tau$, $\Delta_z = c\tau$ yields

$$\left| \frac{\Pi(\phi; \tau, \Delta_x, \Delta_y, \Delta_z)(x, y, z) - \phi(x, y, z)}{\tau} - H(x, y, z, D\phi(x, y, z)) \right| \leq MC \|D^2\phi\| \tau,$$

where $C = a + b + c$. \square

Thus, the operator given by (14) satisfies the conditions of Theorems 1 and 2.

6. Control procedure

In this section, the computation of optimal controls for system (5) according to the extremal aiming procedure is described.

Let ε be a small positive number, t_n the current time instant. Consider a cubic ε -neighborhood

$$\mathcal{U}_\varepsilon = \left\{ (x, y, z) \in R^3 : |x - x(t_n)| \leq \varepsilon, |y - y(t_n)| \leq \varepsilon, |z - z(t_n)| \leq \varepsilon \right\}$$

of the current state $(x(t_n), y(t_n), z(t_n))$ of system (5). By searching through all grid points $(x_i, y_j, z_k) \in \mathcal{U}_\varepsilon$, find the point (x_i, y_j, z_k) such that

$$V^n(x_i, y_j, z_k) = \min_{(x_i, y_j, z_k) \in \mathcal{U}_\varepsilon} V^n(x_i, y_j, z_k).$$

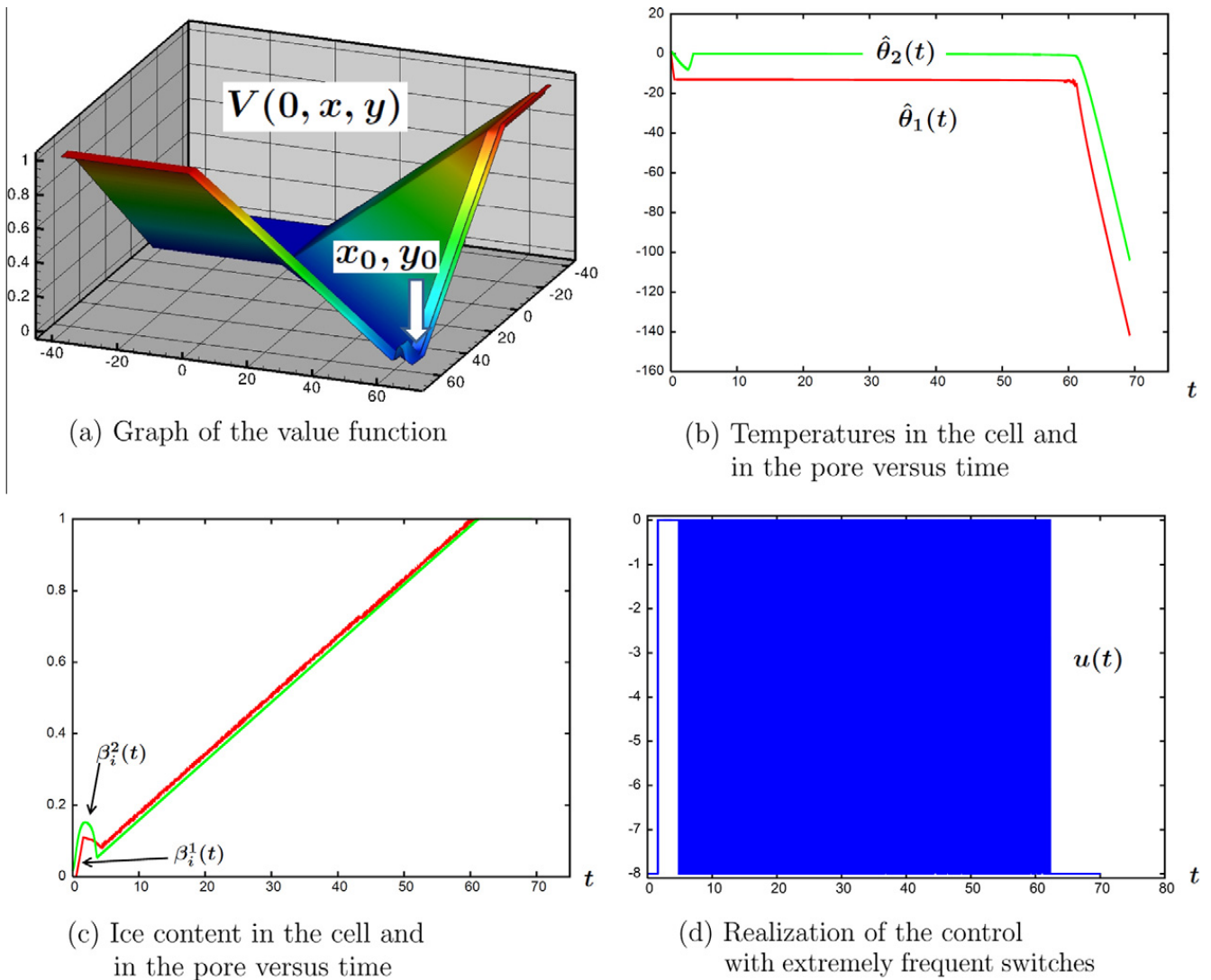


Fig. 10. The case of infinite cooling rate and functional J_2 . Here $\theta_{1s} - \theta_{2s} = -13^\circ \text{C}$.

The current control $u(t_n)$ which is supposed to be applied on the next time interval $[t_n, t_n + \tau]$ is computed from the condition of maximizing the projection of the system velocity (f_1, f_2, f_3) onto the direction of the vector $(x_i - x(t_n), y_i - y(t_n), z_i - z(t_n))$, i.e.

$$u(t_n) = \arg \max_{u \in [-\mu, 0]} ((x_i - x(t_n))f_1 + (y_i - y(t_n))f_2 + (z_i - z(t_n))f_3).$$

It is clear that the value of the control is either 0 or $-\mu$.

Based on the results of [12–14], one can prove that the above discrete control procedure ensures the following estimate. Let $h = \max\{\Delta_x, \Delta_y, \Delta_z\}$. There exist constants C_1 and C_2 such that

$$\int_{t_0}^{t_f} \sigma(x(t), y(t), z(t)) dt < V(t_0, x(t_0), y(t_0), z(t_0)) + C_1(t_f - t_0)\varepsilon,$$

if $C_2 h < \varepsilon$ and $C_2 \sqrt{\tau} < \varepsilon$.

A similar estimate holds for the functional J_2 .

7. Simulation results

First, set $z \equiv u$ and omit the last equation in (5) to obtain the following two-dimensional controlled system that describes the case of infinite cooling rate:

$$\begin{aligned} \dot{x} &= -\alpha_1[\Theta_1(x) - \Theta_2(y)] - \lambda[\Theta_1(x) - u] - d + v_1 \\ \dot{y} &= -\alpha_2[\Theta_2(y) - \Theta_1(x)] + v_2. \end{aligned} \tag{15}$$

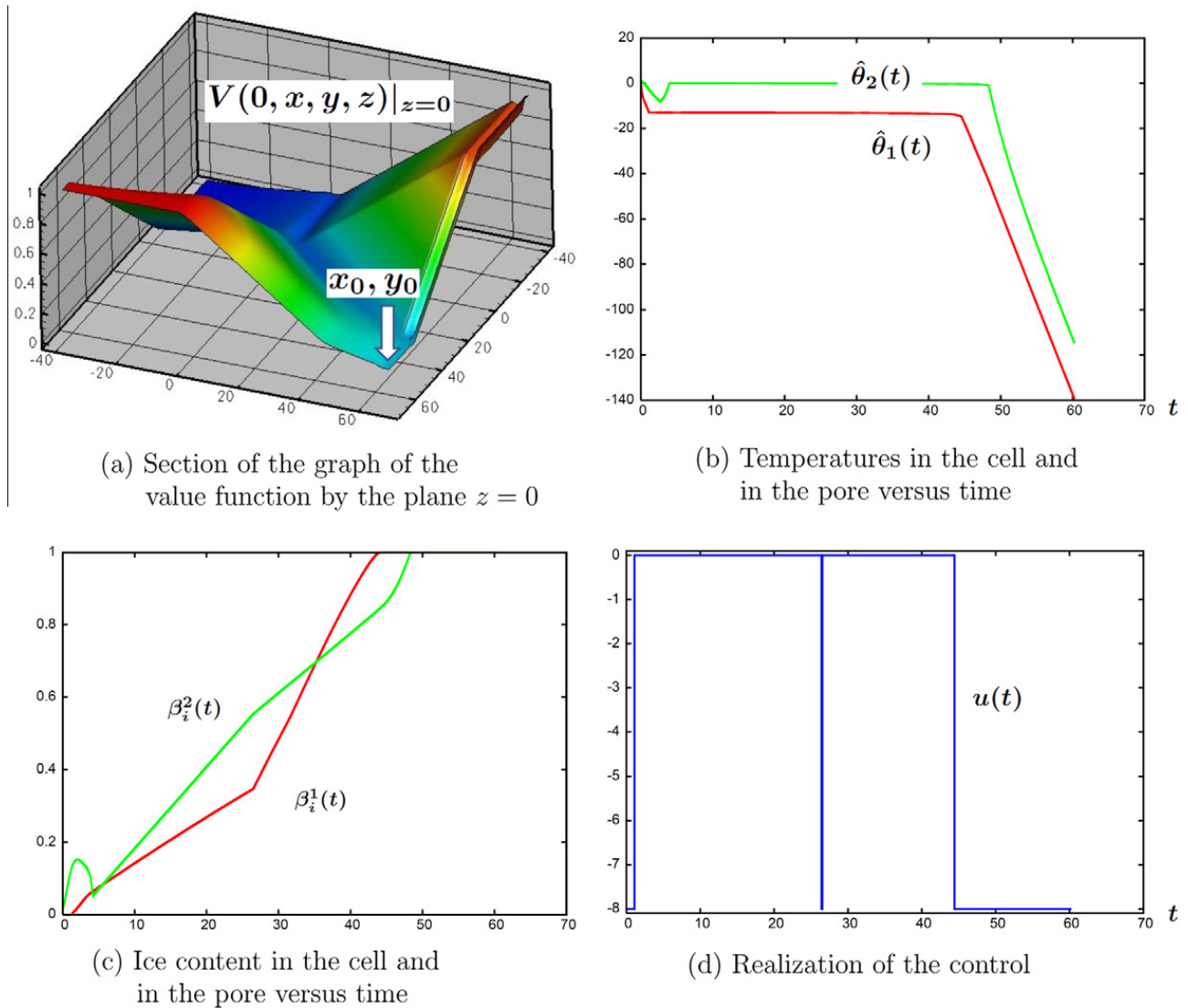


Fig. 11. The case of finite cooling rate and functional J_2 . Here $\theta_{1s} - \theta_{2s} = -13$ °C.

The values of the coefficients and bounds on the control and disturbances are $\alpha_1 = \alpha_2 = 0.1$, $\lambda = 2$, $d = 2$, $\mu = 8$, and $\nu = 0.2$ for all simulations. The functions $\beta_i^k(\theta) := 1 - \beta_i^k(\theta)$, $k = 1, 2$, show the ice fraction in the extracellular and intracellular liquids, respectively.

We start with the case where the intracellular and extracellular liquids have the same freezing temperatures i.e. $\theta_{1s} = \theta_{2s}$. The graph of the value function computed at the time instant $t = 0$ (note that $t_f = 90$) in the case of functional J_1 is shown in Fig. 6(a). The plots of the temperatures in the cell and in the extracellular space versus time are given in Fig. 6(b). Fig. 6(c) shows that the control is not able to bring together the ice contents in the pore and in the cell.

The next simulations are related to the case of different freezing temperatures in the extra- and intracellular spaces: $\theta_{1s} - \theta_{2s} = -13$ °C. The effect of supercooling of the intracellular liquid is manifested as a kink in the dependence of the temperature on the internal energy (see Fig. 7(a) for an experimentally measured curve). In the computations, some idealized curve presented in Fig. 7(b) is utilized.

Fig. 8(a)–(c) give the graph of the value function, the temperatures, and the ice contents, respectively. Comparing Figs. 8a and 6a, one can see that the value function at the start point (x_0, y_0) is much smaller in the case of different freezing temperatures. The control with very frequent switches which is able to equalize the ice contents inside and outside the cell (see Fig. 8(c)) is shown in Fig. 8(d).

Computation results related to the functional J_1 and to system (5) that models finite cooling rates are presented in Fig. 9(a)–(d). Also in this more realistic case, the control ensures keeping the ice contents in the cell and in the extracellular space very close to each other. Note that the computation here is performed in three dimensions. The section of the graph of the value function by the plane $z = 0$ is shown in Fig. 9(a). For this simulation, we have also computed the integral $\int_0^{t_f} |c_{in}(t) - c_{out}(t)| \beta_i^1 \beta_i^2 dt$ that estimates the outflow from the cell during freezing. Such a value obtained using the optimal cooling protocol is approximately 2.7 times less than the one produced by a reasonable heuristic cooling regime. We do

not present the graph of the realization of the heuristic regime because it is very similar to that shown in Fig. 9(d) with the exception that there is only one switch (from -8 to 0) that happens at $t = 1.512$. Note that the final switch (from 0 to -8) in the optimal cooling protocol occurs at $t = 60.8$, i.e. shortly before complete freezing of intracellular and extracellular liquids.

Figs. 10 and 11 correspond to the functional J_2 and the case $\theta_{1s} - \theta_{2s} = -13$ °C. The case of infinite cooling rate is shown in Fig. 10, whereas Fig. 11 displays the case of finite cooling rate. Fig. 11(a) shows the section of the graph of the value function by the plane $z = 0$. In the case of infinite cooling rate, the achieved balance between the ice contents inside and outside the cell is practically identical to that computed using the functional J_1 (compare Fig. 10(c) with Fig. 8(c)). In the case of finite cooling rate, it is even slightly better (compare Fig. 11(c) with Fig. 9(c)).

8. Conclusion

A mathematical model proposed in this paper for the description of competitive intra- and extracellular ice formation can be used to improve cooling protocols utilized in cryopreservation of living cells. The model can be fitted to different cell types by means of the corresponding identification of parameters. The problem is formulated as a differential game in two- or three-dimensional state spaces. A finite difference scheme is applied to compute the value function of the game. All examples presented in this paper are calculated on a Linux computer admitting 32 threads. The coefficient of the parallelization is 0.8 pro thread (25 times totally). The grid size in three dimensions is $300 \times 300 \times 300$, the number of time steps is 30,000 (see a restrictive relation between the space and time steps given by Lemma 1). The run time is approximately 20 min in three-dimensional cases.

The authors already have experiences in the implementation of optimized cooling protocols in Freezer Ice-Cube 15 M plants produced by the firm Sy-Lab Geräte GmbH, Austria. The freezer Ice-Cube 15 M is designed for controlled freezing of samples potted into plastic ampoules. The main part of the plant is a freezing chamber containing a cooling system based on gas nitrogen, a rack for placing ampoules, and two temperature sensors that measure the temperature in the chamber and in the sample, respectively. The plant is supplied with a computer that allows the user to input a cooling profile either manually or as a file prepared in off-line regime. The computer forces the chamber temperature to track the cooling profile using the cooling system. Optimized cooling protocols have been obtained from a simple thermodynamical model see [7] based on averaged values of parameters. The aim of optimization was to reduce the irregular behavior of the temperature caused by the latent heat release and crystallization. Experiments performed on small tissues samples have shown the efficiency of the optimization. The present paper extends that model and proposes a way for the enhancement of cooling protocols.

References

- [1] M. Toner, E.G. Cravalho, M. Karel, Thermodynamics and kinetics of intracellular ice formation during freezing of biological cells, *J. Appl. Phys.* 67 (3) (1990) 1582–1593.
- [2] J.O.M. Karlsson, E.G. Cravalho, M. Toner, A model of diffusion-limited ice growth inside biological cells during freezing, *J. Appl. Phys.* 75 (9) (1994) 4442–4455.
- [3] A.I. Zhmakin, Physical aspects of cryobiology, *Phys.-Usp.* 51 (3) (2008) 231–252.
- [4] G. Caginalp, An analysis of a phase field model of a free boundary, *Arch. Rat. Mech. Anal.* 92 (1986) 205–245.
- [5] Ying Xu, J.M. McDonough, K.A. Tagavi, Dayong Gao, Two-dimensional phase-field model applied to freezing into supercooled melt, *Cell Preserv. Technol.* 2 (2) (2004) 113–124.
- [6] K.-H. Hoffmann, Jiang Lishang, Optimal control of a phase field model for solidification, *Numer. Funct. Anal. Optim.* 13 (1 and 2) (1992) 11–27.
- [7] N.D. Botkin, K.-H. Hoffmann, Optimal control in cryopreservation of cells and tissues, *Adv. Math. Sci. Appl.* 29 (2008) 177–200.
- [8] M. Frémond, *Non-Smooth Thermomechanics*, Springer, Berlin, 2002.
- [9] T.R. Goodman, The heat balance integral and its application to problems involving a change of phase, *Trans. ASME* 80 (1958) 335–342.
- [10] J. Crank, *Free and Moving Boundary Problems*, Clarendon Press, Oxford, 1984.
- [11] Jayme Tchir, Jason Acker, Mitochondria and membrane cryoinjury in micropatterned cells: Effects of cell–cell interactions, *Cryobiology* 61 (2010) 100–107.
- [12] N.N. Krasovskii, A.I. Subbotin, *Positional Differential Games*, Nauka, Moscow, 1974 (in Russian).
- [13] N.N. Krasovskii, *Control of a Dynamic System. The Minimum Problem of a Guaranteed Result*, Nauka, Moscow, 1985 (in Russian).
- [14] N.N. Krasovskii, A.I. Subbotin, *Game-Theoretical Control Problems*, Springer, New York, 1988.
- [15] A.I. Subbotin, A.G. Chentsov, *Optimization of Guaranteed Result in Control Problems*, Nauka, Moscow, 1981 (in Russian).
- [16] A.I. Subbotin, *Generalized Solutions of First Order PDEs*, Birkhäuser, Boston, 1995.
- [17] M.G. Crandall, P.L. Lions, Viscosity solutions of Hamilton–Jacobi equations, *Trans. Amer. Math. Soc.* 277 (1983) 1–47.
- [18] M.G. Crandall, L.C. Evans, P.L. Lions, Some properties of viscosity solutions of Hamilton–Jacobi equations, *Trans. Amer. Math. Soc.* 282 (1984) 487–502.
- [19] M.G. Crandall, P.L. Lions, Two approximations of solutions of Hamilton–Jacobi equations, *Math. Comput.* 43 (1984) 1–19.
- [20] N.D. Botkin, Approximation schemes for finding the value functions for differential games with nonterminal payoff functional, *Analysis* 14 (2) (1994) 203–220.
- [21] P.E. Souganidis, Approximation schemes for viscosity solutions of Hamilton–Jacobi equations, *J. Differ. Eqn.* 59 (1985) 1–43.
- [22] O.A. Malafeyev, M.S. Troeva, A weak solution of Hamilton–Jacobi equation for a differential two-person zero-sum game, in: *Preprints of the Eight Int. Symp. on Differential Games and Applications*, Maastricht, Netherland, July 5–7, 1998, pp. 366–369.
- [23] R. Isaacs, *Differential Games*, John Wiley, New York, 1965.